

Polymer ejection from bacteriophages is fully determined by confinement energy

J. Piili¹ and R. P. Linna^{1,*}

¹Department of Information and Computer Science, Aalto University, P.O. Box 15400, FI-00076 Aalto, Finland

The ejection dynamics through a nanoscale pore of a flexible polymer that is initially strongly confined inside a spherical capsid is examined. By extensive simulations using the stochastic rotation dynamics method we show that the time for an individual monomer to eject grows exponentially with the number of ejected monomers under constant initial monomer density. This dependence is a consequence of the excess free energy of the polymer due to confinement growing exponentially with the initial monomer number inside the capsid, which we address to strong monomer-monomer interactions. Consequently, for sufficiently strong initial confinement and long polymers ejection times for polymers of different lengths depend linearly on the length. At polymer lengths amenable to computer simulations the dependence is superlinear due to the finite-size effect related to the retraction of polymer tails at final stages of ejection.

PACS numbers: 87.15.A-, 82.35.Lr, 87.15.A

Processes involving macromolecules in confinements are studied intensely due to their significance in biology and potential technological and medical applications. An important class of such processes is the capsid ejection where a polymer is initially in a compact conformation inside a capsid and then ejects outside through a pore a few nanometers wide. By far the most important biological process of this class is the viral packaging in and ejection from bacteriophages [1–9].

In the bacteriophages found *in vivo* the viral DNAs are packed to almost crystalline densities [3], realization of which is beyond most molecular-dynamics-based (MD) computer simulations. Computational investigations of some specific characteristics using close-to-realistic model polymers packed to high densities are typically done using some form of probabilistic Metropolis sampling, see *e.g.* [10]. While the studies of the effect and dominance of the different interactions are definitely of high importance, it is disturbing that not even the generic model of a flexible chain ejecting a spherical capsid is completely understood.

In an early work ejection of a flexible polymer starting from a random conformation inside a capsid was investigated by Monte Carlo (MC) simulations [1]. Assuming the excess energy due to the confinement to be $\Delta F/k_B T \sim N_0/R_0^{1/\nu}$ a scaling prediction for the ejection time of the form $\tau \sim N_0 R_0^{1/\nu} = N_0 (N_0/\rho_0)^{1/3\nu}$ was obtained, where N_0 is the degree of polymerization, R_0 the capsid radius, ρ_0 the initial monomer density in the capsid, and ν the Flory exponent. This scaling was confirmed by MC simulations. In a later work [7] the excess energy due to spherical confinement was taken to follow the scaling $\Delta F/k_B T \sim (R_0/R_G)^{3/(3\nu-1)} \sim N_0 \phi^{1/(3\nu-1)}$, where $\phi_0 = N_0 a^3 / R_0^3$ is the initial monomer volume fraction. This scaling law, first introduced by Grossberg and Khokhlov [11], was shown to be correct for the spherically confined polymer at ϕ_0 where the blob scaling in the semidilute conditions is valid [12]. This led to the scaling relation $\tau \sim N_0^{1+\nu} \phi_0^{1/(1-3\nu)}$, again confirmed by MC simulations.

A unified framework for polymer decompression processes was presented by Sakaue and Yoshinaga [8]. Assuming uniform polymer conformation the excess confinement energy inside a spherical capsid was derived in the same form as in [11],

$$\Delta F/k_B T \approx \left(\frac{a}{R_0}\right)^{3/(3\nu-1)} N(t)^{3\nu/(3\nu-1)}. \quad (1)$$

The resultant osmotic driving force $\sim k_B T/\xi(t)$ is exerted on the monomer residing at the pore. The overall dissipation takes place close to the pore, within the range of the correlation length $\xi(t)$, where there exists a velocity gradient of segments of the order $\sim a N(t)/\xi(t)$. Accordingly, the dissipation term was evaluated as $T \dot{S}(t) = \eta [\dot{N}(t)/\xi(t)]^2 \xi(t)^3$. The excess confinement energy is dissipated at the rate $\Delta \dot{F}(t) = -T \dot{S}(t)$, from which the time evolution was obtained as

$$N(t) = N_0 (1 + t/\tau_1)^\beta, \quad (2)$$

where the exponent $\beta = (1 - 3\nu)/[2(1 - \nu)]$ and the time constant $\tau_1 \simeq \tau_0 \phi_0^{(1+\nu)/(1-3\nu)} N_0$. $\tau_0 \simeq \eta a^3 / (k_B T)$ is the monomer scale time constant, where η is the solution viscosity. For the osmotically driven part the scaling $\tau \sim \tau_0 \phi_0^{-(\nu+2)/(3\nu)} N_0^{(2+\nu)/(3\nu)}$ was obtained. [8]

In the present paper the ejection dynamics is explored at larger volume fractions than in the research cited above. Again, we obtain scaling of τ with N_0 . However, the waiting times, *i.e.* the time each monomer, labeled s , has to wait at the pore opening on average to be ejected, are seen not to scale with s . Since the ejection time is just the integral of the waiting time over all the monomers, $\tau = \int_0^{N_0} t_w(s) ds$, where the bead s at the pore is taken as the *reaction coordinate* for the process, polymer ejection is not inherently a scale-invariant process. This is in stark contrast with polymer translocation, where the major part of the waiting time profile scales with s .

The aim of this paper is to show that the dynamics of the ejection process that comprises two parts, the osmotically driven and the diffusive part, as presented within the unified framework [8], is already for fairly moderate initial monomer densities completely determined by the form of the excess energy due to confinement. In other words the scaling expected from the diffusive part does not show in the ejection time.

* Corresponding author: riku.linna@aalto.fi

In what follows, we first briefly describe the computational stochastic rotation dynamics (SRD) method and the capsid and polymer models. In SRD hydrodynamics in the solvent can be switched on and off. For clarity, we present results for polymers that are immersed in Brownian heat bath and report our results on the effect of hydrodynamics in a forthcoming paper [13]. Finally, we summarize our conclusions on the generic polymer ejection process.

We use a hybrid computational method where the time-integration of the polymer is performed by MD implemented by the velocity Verlet (vV) algorithm [14, 15]. The polymer is immersed in a solvent that, in turn, is modeled by SRD [16, 17]. The spherical capsid is modeled as a shell with rigid walls imposing slip and no-slip boundary conditions for polymers and solvent, respectively. The pore is modeled as a cylindrical hole in the shell. The simulation geometry and snapshots of an ejecting polymer are depicted in Fig. 1. The capsid geometry was created using constructive solid geometry technique [18]. The pore radius R_p is 0.4 for the polymer and 0.8 for the solvent. This geometry allows a smooth flow for the solvent bounded by no-slip conditions. The thickness of the capsid wall is 3.

The polymer is modeled as a chain of point-like beads with mass m_b . Adjacent beads are connected via the FENE potential $U_F = -\frac{K}{2}r_{\max}^2 \ln \left(1 - \left(\frac{r}{r_{\max}} \right)^2 \right)$, $r < r_{\max}$, where r is the distance between adjacent beads and K and r_{\max} are potential parameters describing the strength and maximum distance limit of adjacent beads. A Lennard-Jones potential acts between all beads: $U_{LJ} = 4.8\epsilon \left[\left(\frac{\sigma}{r_{ij}} \right)^{12} - \left(\frac{\sigma}{r_{ij}} \right)^6 \right] + 1.2\epsilon$ for $r_{ij} \leq \sqrt[6]{2}\sigma$ and $U_{LJ} = 0$ for $r_{ij} > \sqrt[6]{2}\sigma$. ϵ and σ are potential parameters and r_{ij} is the distance between beads i and j . The potential parameters are chosen as $\sigma = 1.0$, $\epsilon = 1.0$, $K = 30/\sigma^2$, and $r_{\max} = 1.5\sigma$ in reduced units [19].

We use initial monomer density $\rho_0 = N_0 / (\frac{4}{3}\pi R_0^3)$ instead of volume fraction ϕ_0 . Accordingly, the number of monomers N_0 corresponding to $\rho_0 = 1$ is by the factor $\frac{4}{3}\pi$ larger than N_0 corresponding to $\phi_0 = 1$. On the other hand, ϕ_0 was used for hard spheres, the use of which is not possible in high-density MD simulations. A value of ϕ_0 constitutes a slightly lower compression in a system using soft potentials than in one using hard-sphere potentials. This effect is more than compensated by our using ρ_0 instead of ϕ_0 , so effectively the systems simulated here start from more compressed states than those dealt with in [1, 7, 8]. In the initial conformations four beads are inside the pore so the total length of polymers is $N_0 + 4$.

SRD solvent consists of point-like particles whose dynamics can be divided into two steps. In the streaming step the solvent particle positions are moved ballistically, $\vec{r}_i(t + \Delta t) = \vec{r}_i(t) + \vec{v}_i(t)\Delta t$, where t is the simulation time, Δt is the SRD time step, \vec{r}_i is the position, and \vec{v}_i is the velocity of the solvent particle i . The interactions between particles are taken into account in the collision step. The simulation space is divided into a grid of cubic cells of edge length 1.0. There are on average 5 solvent particles per unit cube. To mimic collisions the random parts of velocities of both polymer and solvent particles within each cell are rotated according to the equation

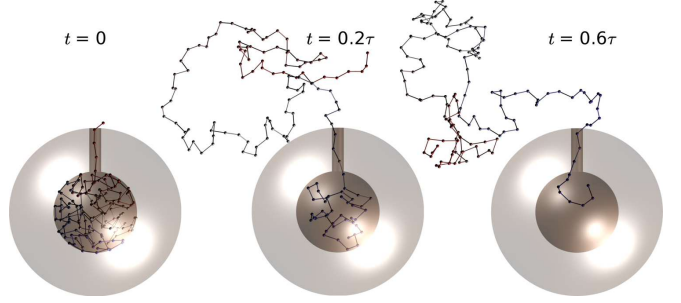


FIG. 1. (Color online) Snapshots of a simulated polymer ejection. (Images created using VMD [21] and POV-Ray [22])

$\vec{v}_i(t + \Delta t) = \vec{v}_{cm}(t) + \Omega [\vec{v}_i(t) - \vec{v}_{cm}(t)]$, where $\vec{v}_{cm}(t)$ is the center-of-mass velocity of the particles in the cell, and Ω is a rotation by angle $\alpha = 3\pi/4$ around an axis that is chosen randomly at each step. In the present case of Brownian heat bath velocities are randomly exchanged between all particles after the collision step. The solvent is kept at the constant temperature of $k_B T = 1.0$ by scaling the random parts of particle velocities, $\vec{v}_i(t) - \vec{v}_{cm}(t)$, such that the equipartition theorem holds at all times. In order to maintain Galilean invariance, the grid is shifted randomly at each time step [20]. The vV time step $\delta t = 0.0002$ and the SRD time step $\Delta t = 0.5$. A relatively small δt in vV is required to prevent numerical errors accumulating inside the capsid when the monomer density is high. MD and SRD steps are performed in turns such that after $\Delta t/\delta t = 2500$ vV steps a single SRD step is performed.

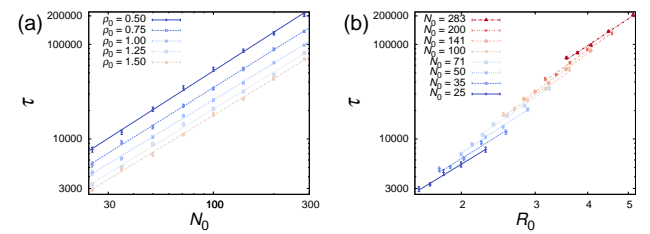


FIG. 2. (Color online) (a) Ejection time τ as a function of polymer length N_0 for different initial monomer densities ρ_0 . The points are averages over 40-50 runs. The lines are the fitted curves of the form $\tau \sim N_0^\beta$. $\beta = 1.362 \pm 0.05$, 1.325 ± 0.04 , 1.293 ± 0.04 , 1.299 ± 0.03 , and 1.300 ± 0.04 for $\rho_0 = 0.5$, 0.75 , 1 , 1.25 , and 1.5 , respectively. (b) τ as a function of capsid radius R_0 for different N_0 , $\tau \sim R_0^\zeta$. From bottom to top: $\zeta = 2.71$, 2.77 , 2.90 , 3.05 , 2.97 , 3.23 , 3.19 , and 2.92 for $N_0 = 25$, 35 , 50 , 71 , 100 , 141 , 200 , and 283 , respectively.

An initial polymer conformation is created by injecting a polymer into the capsid by force at the pore that is ramped up until the desired ρ_0 is reached. The polymer is then thermalized by scaling the bead velocities. During the ejection the polymer maintains its temperature via the SRD solvent collision step.

Fig. 2 (a) shows the ejection time τ vs number of monomers N_0 initially inside the capsid for different initial densities ρ_0 . As reported earlier [1-4, 6-9], scaling $\tau \sim N_0^\beta$ is obtained. $\beta = 1.362 \pm 0.05$, 1.325 ± 0.04 , 1.293 ± 0.04 , 1.299 ± 0.03 ,

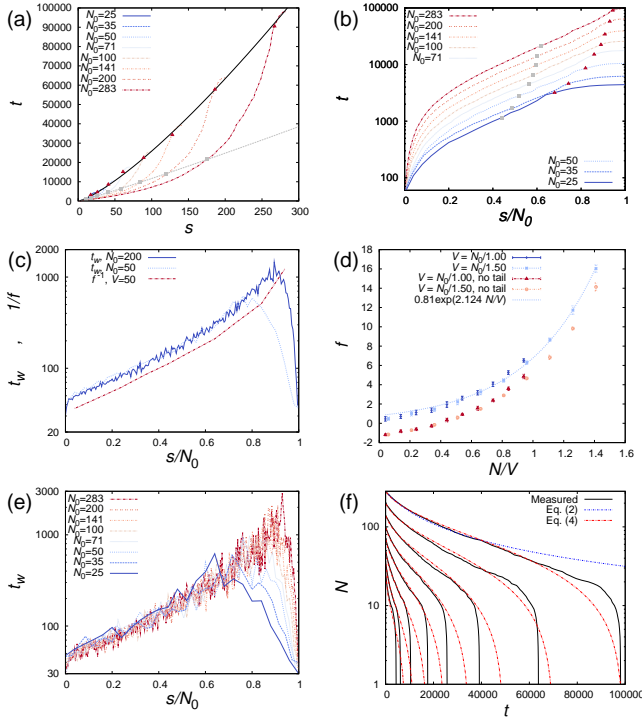


FIG. 3. (Color online) (a) The cumulative waiting time of simulations where $\rho_0 = 1.0$. Averages over 50 runs. The times when the end monomers of polymers of different lengths escape scale as $\tau \sim N_0^{1.29}$ (solid line). Reaction coordinates at instants when the inner part of the polymer exerts no force to the bead at the pore (■): $s(\tau_2^*) \sim s^{1.0866}$ (dotted gray line). Reaction coordinate when number of beads inside the capsid $N = g_0$ (▲) (b) The cumulative waiting time vs normalized reaction coordinate s/N_0 for $\rho_0 = 1.0$ and different N_0 . Squares (■) and triangles (▲) correspond to those in (a). (c) Waiting times t_w for $N_0 = 50$ and 200 and the inverse of the measured force at the pore $1/f$ for $N_0 = 50$. $\rho_0 = 1.0$. $1/f$ scaled by the factor 500. t_w values are averages over 500 runs. (d) Force measured at the pore as a function of N/V , where N is the number of beads inside the capsid and V is the capsid volume. $N_0 = 100$. The lower data points (no tail) depict the force measured without beads outside the capsid. (e) Waiting times t_w for all simulated values of N_0 . Data here is averaged over 50 runs, which results in poorer statistics for the date presented in (c). (f) Beads in the capsid $N(t)$ during the ejection for the same N_0 as in (e) with fits to Eqs. (2) and (4).

and 1.300 ± 0.04 for $\rho_0 = 0.5, 0.75, 1, 1.25$, and 1.5 , respectively. The exponent β decreases slightly with increasing initial monomer density for $\rho_0 \leq 1$ in accordance with our previous findings [9]. This is in accord with what we have stated in the case of driven translocation when the driving bias force increases [23, 24]. The deterministic driving force (pressure) increases with ρ_0 . Most of the effective friction is exerted on the ejecting polymer in the vicinity of the pore through which the pressure pushes it. Hence, with increasing ρ_0 the contribution from driving becomes more dominant over diffusion. As the driving is frictional the dependence can only approach linear, *i.e.* $\tau \sim N_0^\beta$, $\beta \rightarrow 1$. For extremely dense conformations $\rho_0 \geq 1$, β increases with ρ_0 due to the increasing contribution

from the friction between monomers in the capsid. For polymers of $N_0 \geq 50$ $\tau \propto 1/\rho_0$ is obtained very precisely, which is in accordance with the above reasoning. A surface fit to the whole data for different N_0 and ρ_0 gives $\tau \sim \rho_0^\alpha N^\beta$, where $\alpha = -0.980 \pm 0.039$, and $\beta = 1.316 \pm 0.019$.

Fig. 2 (b) shows τ as a function of capsid radius R_0 . Comparing the obtained scaling $\tau \sim R_0^\zeta$, where $\zeta \in [2.71, 3.23]$, with the scaling in Fig. 3 (a) of [8], where ζ decreases from 5 toward 2 when R_0/a decreases from 10^2 toward 1, suggests that the ejection takes place in the very strongly confined regime. We also measured the radii of gyration R_g for the polymers' initial conformations inside the capsids. Spherical scaling $R_g \sim N_0^\theta$, where $\theta \approx 0.33$, was obtained for all ρ_0 also confirming strong confinement.

Although ejection times τ scale with N_0 , as seen from the endpoints of the cumulative waiting times, $t(s)$ as such do not scale with s , but grow exponentially with s , see Figs. 3 (a) and (b). Accordingly, waiting times of the ejecting monomers $t_w = t(s) - t(s-1)$ follow the exponential form, $t_w \sim \exp(As)$, as seen in Fig. 3 (c). This is in accord with the waiting time profile found in [9] for the ejection through a symmetric pore.

As for large enough ρ_0 the waiting time at any time is expected to be largely dominated by the instantaneous pressure inside the capsid driving the ejecting polymer the dependence $t_w \sim \exp(As)$ is at odds with the excess energy due to confinement based on the blob scaling under semidilute conditions, Eq. (1). To rule out the possibility that $t_w(s)$ deviated from what is expected from the semidilute assumption due to the polymer segment outside the capsid being driven out of equilibrium, we measured R_g of this segment at different stages. This proved to be only slightly smaller than the measured corresponding equilibrium R_g scaling as $R_g \sim s^{0.6}$, so monomers do not crowd close to the pore and so change $t_w(s)$.

Fig. 3 (d) shows the force that has to be exerted on the monomer at the pore to keep it in position at different s . Fluctuations at small ρ are large and f - s dependence can be determined only for $\rho \gtrsim 0.2$. This is well above $\phi = 0.1$ where ΔF was seen to deviate from the form predicted by the semidilute blob picture [25]. Force due to confinement was measured also via the change in the momenta of the particles hitting the capsid walls. This way we obtain the force, or pressure, exerted on the whole capsid surface. The force measured this way and at the pore have the same dependence on ρ . We also measured force at the pore for different N for a model with only the polymer segment inside the capsid present and the rest of the polymer removed. f for this modified model has the exact same dependence on s as for the full model, only the force magnitude is less by 2 (see Fig. 3 (d)). Hence, the ejected part of the polymer significantly contributes to the ejection throughout the process but does not essentially change the generic features of dynamics.

The measured force has very precisely the exponential dependency $f \sim \exp[BN(t)]$ anticipated from t_w . In Fig. 3 (c) we plot $1/f$ for the force measured for $\rho_0 = 1$ and $N_0 = 50$. $t_w \propto 1/f$ is seen to hold very precisely for all $s/N_0 \lesssim 0.9$, that is, throughout the ejection until the final retraction of the

monomers remaining in the capsid. The exponential growth arises due to excluded volume interactions: inside the capsid monomers interact individually rather than as ensembles of blobs and the higher order interaction terms become important. This observation is in contrast with the claimed screening of the excluded volume interactions at high concentrations giving rise to a different scaling than given by the semidilute blob picture, Eq. (1) [25].

Using the measured dependence $f = C \exp[BN(t)]$, we can calculate τ as a function of ρ_0 in the framework presented in [8]. If the monomers are packed inside the capsid by force applied at the pore, then the excess energy that results from packing N monomers is $\Delta F \approx \sum_{i=0}^{N-1} f_i \Delta l_i$, where f_i is the force required to move the bead i at the inner pore opening into the capsid and the bead $i+1$ in its place, Δl_i is the distance the bead $i+1$ needs to be moved. In the case of f_i being measured for individual beads $\Delta l_i = a \approx 1, \forall i$. In the limit $\Delta l_i \rightarrow 0$ and the minimum necessary force being applied continuously on the polymer at the inner pore opening $\Delta F = \int_1^N f(n) dn = \int_1^N C \exp(Bn) dn = (C/B)[\exp(BN) - D]$, where B , C , and D are constants. $C \propto k_B T$. From Figs. 3 (c)-(e) it is evident that $B = A/N_0$, where A is a constant. Relating the rate of change of this energy to the overall dissipation (see text after Eq. (1)), $\Delta \dot{F}(t) = -T \dot{S}(t) \approx \eta [a \dot{N}(t)/\xi(t)]^2 \xi(t)^3$, we get

$$\dot{N}(t) = -\frac{C}{\eta a^2 \xi(t)} e^{BN(t)}. \quad (3)$$

Approximating the correlation length to be constant $\xi(t) = \xi$ and using the initial condition $N(t=0) = N_0$, the solution is given in the form

$$N(t) = -\frac{N_0}{A} \ln \left(\frac{AC}{N_0 \eta a^2 \xi} t + e^{-A} \right). \quad (4)$$

Fig. 3 (f) shows the fit of Eq. (4) to the measured $N(t)$. A fit of $N(t)$ given by Eq. (2) for the largest $N_0 = 283$ is given for reference. Eq. (4) is seen to describe $N(t)$ with excellent precision as it should given that $t_w \propto 1/f$ almost throughout the ejection.

To demonstrate that ΔF mainly determines the scaling $\tau \sim N_0^\beta$ for the driven part we apply the criterion from the semidilute picture for the termination of osmotic driving. Let τ_2 be the time when the number of monomers in the capsid has decreased to the number corresponding the relaxed chain conformation of average radius R_0 : $N(t=\tau_2) = g_0 = (R_0/a)^{1/\nu}$. For constant ϕ_0 and different N_0 and R_0 , $g_0 = (N_0/\phi_0)^{1/(3\nu)}$. This gives

$$\begin{aligned} \tau_2 &\approx \frac{N_0 \eta a^2 \xi}{AC} \left[\exp \left(-\frac{A}{N_0} \left(\frac{N_0}{\phi_0} \right)^{\frac{1}{3\nu}} \right) - e^{-A} \right] \\ &\propto \frac{N_0}{k_B T}, \text{ for large } N_0. \end{aligned} \quad (5)$$

τ_2 is seen to grow linearly with N_0 .

We used g_0 as a criterion for a relaxed chain to demonstrate that even with its scaling form the linear relation $\tau \sim N_0$ is

obtained. However, for the volumes that give the initial densities $\rho_0 = 0.5 \dots 1.5$ there would be only a few monomers per blob. The times τ_2 given by $N(t=\tau_2) = g_0$ are marked in Fig. 3 (b). τ_2 are at points where the short remaining tail inside the capsid rapidly retracts through the pore due to the large entropy difference on both sides of the capsid. Clearly, ρ_0 are so large that τ_2 are not relevant. Instead, we can use the times τ_2^* when the measured force exerted by the polymer segment inside the capsid on a monomer at the pore is zero as a criterion for the termination of osmotic driving. Also τ_2^* are marked in Fig. 3 (b). We obtain $N(t=\tau_2^*) \sim N_0$. Again, linear relation $\tau_2^* \sim N_0$ is obtained. From Figs. 3 (c) and (e) it is seen that $t_w(s/N_0)$ for different N_0 deviate from the common form only at the final stage of ejection when the remaining part of the polymer retracts from the capsid. Shorter polymers start retracting at a relatively earlier point in the process. Retraction speed increases identically for all polymers. This results in $\tau \sim N_0^\beta$, where $\beta > 1$. For very strong initial confinement this is a finite-size effect. After τ_2^* the force due to entropic imbalance between polymer segments outside and inside the capsid exerted at the pore causes the tension to propagate from the pore along the polymer segment in the capsid. The tension propagating similarly, the tensed segment Δs will grow identically for all N_0 . Hence, $\Delta s/N_0$ will be larger for smaller N_0 resulting in retraction starting at smaller s/N_0 for shorter polymers. Hence, for asymptotically long polymers linear dependence $\tau \sim N_0$ is obtained. For a weaker initial confinement the exponentially decaying force driving the diffusive polymer segment can give superlinear dependence.

In conclusion, we have investigated in detail the ejection of flexible polymers from spherical capsids through a nanoscale pore. Polymers were simulated by molecular dynamics and the surrounding heat bath by stochastic rotation dynamics. The ejection dynamics and the pertaining excess energy due to confinement ΔF were analyzed via measured waiting time profiles and forces exerted on polymers at the pore. We found that the waiting times t_w , that is, the times it takes for individual monomers to exit the capsid, grow exponentially with the number of ejected monomers. The force f measured at the pore, in turn, increases exponentially with the number of monomers in the capsid N . This we address to follow from ΔF growing exponentially with N due to the higher-order terms in monomer-monomer interactions for the sufficiently high monomer densities. We also found that $t_w \sim 1/f$ holds well for the simulated densities. This means that the form of ΔF completely determines the ejection dynamics for strongly confined polymers. We showed that the dependence $\Delta F \sim \exp(AN/N_0)$ can only give linear dependence for the ejection time on the polymer length $\tau \sim N_0$. For strong initial confinement the apparent scaling $\tau \sim N_0^\beta$, where $\beta > 1$ results from a finite-size effect that is likely related to tension propagation. We have here shown that already for densities far lower than those found in bacteriophages ejection dynamics is fully determined by the form of the excess energy due to confinement that results from strong monomer-monomer interactions. We have also shown that even for densities that are moderate compared to those in bacteriophages no assistance for example by flow is necessary for the ejection to complete.

ACKNOWLEDGMENTS

We thank T. Sakaue for useful comments. The computational resources of CSC-IT Centre for Science, Finland, and Aalto Science-IT project are acknowledged. The work of Joonas Piili is supported by Tekniikan edistämässäätö and The Emil Aaltonen Foundation.

[1] M. Muthukumar *Phys. Rev. Lett.*, vol. 86, p. 3188, 2001.

[2] C. Forrey and M. Muthukumar *Biophys. J.*, vol. 91, p. 25, 2006.

[3] D. E. Smith, S. B. Tans, S. Smith, S. B. Grimes, D. L. Andersen, and C. Bustamante *Nature*, vol. 413, p. 748, 2001.

[4] P. Grayson, L. Han, T. Winther, and R. Phillips *Proc. Natl. Acad. Sci. U.S.A.*, vol. 104, p. 14652, 2007.

[5] I. Ali, D. Marenduzzo, and J. M. Yeomans, “Polymer packaging and ejection in viral capsids: Shape matters,” *Phys. Rev. Lett.*, vol. 96, p. 208102, 2006.

[6] S. Ghosal *Phys. Rev. Lett.*, vol. 109, p. 248105, 2012.

[7] A. Cacciuto and E. Luijten, “Confinement-driven translocation of a flexible polymer,” *Phys. Rev. Lett.*, vol. 96, p. 238104, 2006.

[8] T. Sakaue and N. Yoshinaga, “Dynamics of polymer decompression: Expansion, unfolding, and ejection,” *Phys. Rev. Lett.*, vol. 102, p. 148302, Apr 2009.

[9] R. P. Linna, J. E. Moisio, P. M. Suhonen, and K. Kaski, “Dynamics of polymer ejection from capsid,” *Phys. Rev. E*, vol. 89, p. 052702, May 2014.

[10] D. Marenduzzo, C. Micheletti, E. Orlandini, and D. W. Sumners, “Topological friction strongly affects viral dna ejection,” *Proceedings of the National Academy of Sciences*, vol. 110, no. 50, pp. 20081–20086, 2013.

[11] A. Y. Grosberg and A. R. Khokhlov, *Statistical Physics of Macromolecules*. New York: American Institute of Physics, 1994.

[12] T. Sakaue and E. Raphaël *Macromolecules*, vol. 39, p. 2621, 2006.

[13] Piili, J. and Linna, R. P., to be submitted to *Phys. Rev. E*.

[14] W. C. Swope, H. C. Andersen, P. H. Berens, and K. R. Wilson, “A computer simulation method for the calculation of equilibrium constants for the formation of physical clusters of molecules: Application to small water clusters,” *The Journal of Chemical Physics*, vol. 76, no. 1, pp. 637–649, 1982.

[15] D. Frenkel and B. Smit, *Understanding molecular simulation: from algorithms to applications*. Academic Press, 2001.

[16] A. Malevanets and R. Kapral, “Mesoscopic model for solvent dynamics,” *J. Chem. Phys.*, vol. 110, pp. 8605–8613, 1999.

[17] A. Malevanets and R. Kapral, “Mesoscopic multi-particle collision model for fluid flow and molecular dynamics,” *Novel Methods in Soft Matter Simulations*, vol. 149, pp. 2258–2266, 2004.

[18] G. Wyvill and L. Kunii, T., “A functional model for constructive solid geometry,” *The Visual Computer*, vol. 1, p. 3, 1985.

[19] M. P. Allen and D. J. Tildesley, *Computer Simulation of Liquids*. Oxford: Clarendon Press, 2006.

[20] T. Ihle and D. M. Kroll, “Stochastic rotation dynamics: A galilean-invariant mesoscopic model for fluid flow,” *Phys. Rev. E*, vol. 63, p. 020201, Jan 2001.

[21] W. Humphrey, A. Dalke, and K. Schulten, “VMD – Visual Molecular Dynamics,” *Journal of Molecular Graphics*, vol. 14, pp. 33–38, 1996.

[22] Persistence of Vision Pty. Ltd., “Persistence of Vision (TM) Raytracer (Version 3.6),” 2004. [Computer software].

[23] V. V. Lehtola, R. P. Linna, and K. Kaski, “Dynamics of forced biopolymer translocation,” *EPL*, vol. 85, p. 58006, 2009.

[24] V. V. Lehtola, R. P. Linna, and K. Kaski *Phys. Rev. E*, vol. 78, p. 061803, 2008.

[25] A. Cacciuto and E. Luijten, “Self-avoiding flexible polymers under spherical confinement,” *Nano Letters*, vol. 6, p. 901, 2006.